IEEE Access
Multidisciplinary ⋮ Rapid Review ⋮ Open Access Journal

Received October 13, 2020, accepted October 17, 2020, date of publication October 26, 2020, date of current version November 9, 2020.

Digital Object Identifier 10.1109/ACCESS.2020.3033892

Improved-Efficacy Optimization of Compact Microwave Passives by Means of Frequency-Related Regularization

SLAWOMIR KOZIEL[1,2], (Senior Member, IEEE),
ANNA PIETRENKO-DABROWSKA[2], (Senior Member, IEEE),
AND MUATH AL-HASAN[3], (Senior Member, IEEE)

[1]Engineering Optimization and Modeling Center, Department of Technology, Reykjavik University, 101 Reykjavik, Iceland
[2]Faculty of Electronics, Telecommunications and Informatics, Gdansk University of Technology, 80-233 Gdańsk, Poland
[3]Networks and Communication Engineering Department, Al Ain University, Al Ain, United Arab Emirates

Corresponding author: Anna Pietrenko-Dabrowska (anna.dabrowska@pg.edu.pl)

This work was supported in part by the Rannsóknamiðstöð Icelandic Centre for Research (RANNIS) under Grant 206606051, in part by the National Science Centre of Poland under Grant 2018/31/B/ST7/02369, and in part by the Abu-Dhabi Department of Education and Knowledge (ADEK) Award for Research Excellence 2019 under Grant AARE19-245.

ABSTRACT Electromagnetic (EM)-driven optimization is an important part of microwave design, especially for miniaturized components where the cross-coupling effects in tightly arranged layouts make traditional (e.g., equivalent network) representations grossly inaccurate. Efficient parameter tuning requires reasonably good initial designs, which are difficult to be rendered for newly developed structures or when re-design for different operating conditions or material parameters is required. If global search is needed, due to either the aforementioned issues or multi-modality of the objective function, the computational cost of the EM-driven design increases tremendously. This paper introduces a frequency-related regularization as a way of improving the efficacy of simulation-based design processes. Regularization is realized by enhancing the conventional (e.g., minimax) objective function using a dedicated penalty term that fosters the alignment of the circuit characteristics (e.g., the operating frequency or bandwidth) with the target values specified by the design requirement. This leads to smoothening of the objective function landscape, improves reliability of the optimization process, and reduces its computational cost as compared to the standard formulation. An added benefit is the increased immunity to poor initial designs and multi-modality issues. In particular, regularization can make local search routines sufficient in situations where global optimization would normally be necessary. The presented approach is validated using two miniaturized circuits, a rat-race and a branch line coupler. The numerical results demonstrate its superiority over conventional design problem formulations in terms of reliability of the optimization process.

INDEX TERMS Microwave design, miniaturized passive components, design optimization, EM-driven design, gradient-based search, regularization.

I. INTRODUCTION

Although the development of microwave circuits traditionally relies on theoretical and equivalent network models [1]–[4], the importance of electromagnetic (EM)-driven design has been continuously growing over the years [5], [6]. On the one hand, EM analysis is indispensable for reliable performance evaluation that accounts for the phenomena that cannot be reliably quantified by simpler representations [7]. On the other hand, simulation models are frequently used in the design process itself, e.g., for tuning geometry parameters [8] or uncertainty quantification [9], [10]. EM-based design tasks are solved using numerical optimization [11] and modelling methods [12], which is mainly due to inadequacy of traditional EM-based techniques (e.g., supervised parameter sweeping) that are unable to handle multiple parameters, performance requirements, and constraints. Miniaturized microwave passives are representative examples of structures where EM-driven design closure is mandatory due to a typically large—compared to conventional

The associate editor coordinating the review of this manuscript and approving it for publication was Liang-Bi Chen.

This work is licensed under a Creative Commons Attribution 4.0 License. For more information, see https://creativecommons.org/licenses/by/4.0/

transmission line (TL)-based circuits—number of geometry parameters, and strong cross-coupling effects being a result of the employment of TL folding [13] or compact building blocks involving slow-wave phenomenon [14] (e.g., compact microwave resonant cells, CMRCs [15]). For such structures, circuit-theoretical methods are only capable of yielding initial designs that need further tuning to meet the design goals imposed on their electrical characteristics.

As elaborated on above, EM-driven design optimization of microwave components is necessary but also challenging. While the cost of individual full-wave simulation of a particular design is not a problem, massive analyses required by the optimization procedures may become a practical obstacle. This is usually not a serious problem for local search procedures (e.g., gradient-based [16], or pattern search algorithms [17]) assuming that the initial design is of sufficient quality. Nevertheless, handling poor initial designs, or multi-modal cases featuring multiple local optima is typically a more expensive endeavour because of involving global optimization routines, e.g., population-based metaheuristics [18], [19], [21]. Similar issues arise when solving tasks such as multi-objective optimization [22]–[25], or uncertainty quantification (statistical analysis [26], yield-driven design [27]–[29]). Clearly, the advancements in computer hardware and simulation software mitigates these difficulties to a certain extent. Notwithstanding, these are often outweighed by the ever increasing demands for improved evaluation reliability (e.g., by accounting for phenomena such as substrate anisotropy [30] or multi-physics effects [31]) as well as the need for simulating more and more complex systems.

Given the aforementioned challenges, it is no surprise that the development of methods for accelerating EM-driven design procedures has been widely researched over the last decades. The available techniques include gradient-based routines expedited by adjoint sensitivities [32], [33] or sparse Jacobian updates [34], [35], as well as surrogate-assisted algorithms involving approximation models [36]–[38] and variable-fidelity simulations [39]–[41]. A representative example of the latter is space mapping [42] widely used in microwave engineering [43]. Others include response correction methods, e.g., manifold mapping [44] or adaptive response scaling [45]. Popular solutions for global search are data-driven surrogates [46] and machine learning techniques [47], often combined with sequential sampling procedures [48], where construction of the surrogate is interleaved with prediction stages leading to a generation of infill points and identifying the promising regions of the search space [49]. Robust design can be also aided by approximation surrogates, with a notable example of polynomial chaos expansion (PCE) models [27], which have the advantage of estimating the statistical moments of the system outputs without the necessity of running Monte Carlo analysis [50].

From the perspective of frequency characteristics of the system and their manipulation through numerical optimization procedures, the primary challenge is an appropriate alignment of the poles/zeros, resonances, or the circuit passband, with the target operating frequencies. The difficulty arises from the fact that shifting the sharp slopes of the characteristic is significantly more difficult than vertical (level) adjustment, especially when the design specifications are defined in a minimax form [51]. One of the consequences is that global optimization routines may need to be launched in the case of poor initial designs (e.g., the operating frequency being too far away from the target one). The methods such as feature-based optimization (FBO) [52] or transfer function zero/pole tracking [53] can be used as a workaround yet these methods are problem dependent. For example, feature point definition in FBO has to be tailored to a particular type of characteristic [54], whereas identification of the transfer function poles and zeros requires vector fitting [55], which may face uniqueness problems.

This paper discusses a frequency-related regularization approach, which is developed to alleviate the difficulties mentioned in the previous paragraph. It is realized by complementing the objective function pertinent to the design problem at hand with a special penalty term that quantifies the discrepancies between the actual and the target operating frequency (or frequencies in the case of multi-band structures). The contribution of this term enforces the frequency alignment but it does not modify the original cost function when close to the optimum. Its analytical form is designed to smoothen the functional landscape handled by the optimization routine. In particular, it can make the optimum reachable by the local algorithms even in situations that normally call for using global procedures. An additional benefit is reduction of the computational cost of the optimization process. Our methodology is demonstrated using two compact microstrip couplers and compared to conventional optimization that does not use regularization. The results obtained for various design scenarios and a range of performance specifications corroborate the efficacy of the technique and the importance of regularization for improving reliability of the optimization process.

II. FREQUENCY REGULARIZATION FOR ACCELERATED MICROWAVE DESIGN OPTIMIZATION

The purpose of this section is to formulate and explain the regularization scheme for microwave design optimization. It should be emphasized that regularization is not an optimization procedure by itself but it is a modification of the objective function in a way that facilitates the relocation of the frequency characteristics of the device at hand according to performance specifications imposed onto the system. Hence, it can work with any numerical routine of choice. In this paper, the trust-region gradient search is employed as the primary optimization algorithm.

A. PROBLEM FORMULATION

The computational (here, EM-simulated) model of the microwave component under optimization will be denoted as $S(\boldsymbol{x})$, where $\boldsymbol{x}$ is a vector of independent design parameters,

whereas S stands for the relevant system outputs, typically, S-parameters and the quantities derived from them (e.g., the phase shift of a coupler [56]). We will also use the notation $S_{kj}(\boldsymbol{x},f)$, where k and j denote the component ports and f is a frequency. In the cases of microwave couplers, we are mainly interested in the following characteristics: matching $S_{11}(\boldsymbol{x},f)$, transmission $S_{21}(\boldsymbol{x},f)$ and $S_{31}(\boldsymbol{x},f)$, and isolation $S_{41}(\boldsymbol{x},f)$. The design quality is evaluated using a merit function $U(S(\boldsymbol{x}))$, defined so it decreases for designs that are better with respect to the assumed performance specifications. The optimization task is formulated as

$$\boldsymbol{x}^* = \arg\min_{\boldsymbol{x}} U(S(\boldsymbol{x})) \tag{1}$$

In (1), $\boldsymbol{x}^*$ is the optimum design ensuring minimum of the merit function U to be identified, and $S(\boldsymbol{x})$ denotes the system response at the design $\boldsymbol{x}$. A particular form of the merit function is problem dependent. For example, if the goal is to improve the matching of the impedance transformer over a bandwidth determined by the lower and upper frequencies f_L and f_U, respectively, we may have

$$U(S(\boldsymbol{x})) = \max\{f_L \leq f \leq f_U : |S_{11}(\boldsymbol{x},f)|\} \tag{2}$$

where f stands for frequency, the frequencies f_L and f_U delimit the bandwidth B, and $S_{11}(\boldsymbol{x},f)$ refers to the matching characteristics of the device at hand at the design $\boldsymbol{x}$ and frequency f.

As another example, consider a microstrip coupler that is supposed to operate at the frequency f_0 so that both its matching and isolation are better than -20 dB at f_0, and the power split error $d_S(\boldsymbol{x},f) = ||S_{21}(\boldsymbol{x},f)| - |S_{31}(\boldsymbol{x},f)|| \leq 0.5$ dB for the maximum possible symmetric bandwidth centered at f_0. In this case, the merit function may be formulated as

$$U(S(\boldsymbol{x})) = -B(\boldsymbol{x}) + \beta c(\boldsymbol{x})^2 \tag{3}$$

The second term of (3) is the penalty term that allows for ensuring required level of matching and isolation. In (3), β is the penalty coefficient whose value is selected so as to ensure sufficient contribution of a penalty term in case of constraint violation. Whereas $\boldsymbol{c}(\boldsymbol{x})$ is the penalty function defined below. In addition, B is the power split bandwidth defined as

$$B(\boldsymbol{x}) = \begin{cases} 2\min\{f_0 - f_{\min}, f_{\max} - f_0\} & \text{if } d_S(\boldsymbol{x},f_0) \leq 0.5 \text{ dB} \\ 0.5 - d_S(\boldsymbol{x},f_0) & \text{otherwise} \end{cases} \tag{4}$$

In (4), the frequencies $f_{\min}$ and $f_{\max}$ are the minimum and maximum frequency, respectively, that determine the continuous range around the operating frequency f_0 for which the condition on the power split error $d_S(\boldsymbol{x},f) \leq 0.5$ dB is satisfied. Note that if $d_S(\boldsymbol{x},f_0) > 0.5$ dB, the bandwidth is defined as negative and proportional to the violation of the power split condition. This is to ensure monotonicity of the cost function when moving from poor to good designs. The penalty function $c(\boldsymbol{x})$

$$c(\boldsymbol{x}) = \max\left\{\frac{\max\{|S_{11}(\boldsymbol{x},f_0)|, |S_{41}(\boldsymbol{x},f_0)|\} + 20}{20}, 0\right\} \tag{5}$$

quantifies a relative violation of the matching $S_{11}(\boldsymbol{x},f)$ and isolation $S_{41}(\boldsymbol{x},f)$, conditions and contributes to the primary objective, i.e., the bandwidth $B(\boldsymbol{x})$ in case of actual violation of either of these.

B. FREQUENCY-RELATED REGULARIZATION. CONCEPT AND BENEFITS

As explained in the introduction, relocating the circuit characteristics to a different frequency range is challenging from the point of view of numerical optimization. A typical situation is illustrated in Fig. 1 that shows S-parameters of a compact microstrip coupler considered in Section III. The design specifications and the objective function are set up according to (3)-(5) with $f_0 = 1.2$ GHz. At the initial design, the coupler operates at the frequency around 0.6 GHz and its characteristics are severely misaligned. The profile of the objective function (3)-(5) evaluated along the line segment connecting the two designs and shown in Fig. 1(c) indicates a local maximum, which indicates that global search might be necessary. Clearly, the picture is a simplified representation of the issue but it still demonstrates potential challenges when optimizing the structure using numerical routines.

Frequency-related regularization discussed in this work attempts to address this problem by introducing a regularization function $f_r(\boldsymbol{x})$, which quantifies the misalignment betwen the acqual operating frequencies of the circuit and their target values. The function $f_r(\boldsymbol{x})$ is subsequently used to modify the objective function of the problem as follows

$$U_r(S(\boldsymbol{x})) = U(S(\boldsymbol{x})) + \beta_r\left[\max\left\{\frac{f_r(\boldsymbol{x}) - f_{r.\max}}{f_{r.\max}}, 0\right\}\right]^2 \tag{6}$$

In (6), $f_{r.\max}$ is a user-defined maximum allowed misalignment between the actual and the intended operating frequency (or frequencies), β_r denotes a user-defined penalty factor, and f_r refers to is a regularization function whose definition is problem specific (cf. (7). As it can be seen, the regularization term increases the primary objective function in a manner proportional (through a user-defined factor β_r) to the discrepancy level according to f_r. The introduction of $f_{r.\max}$ allows for completely removing the above contribution when close to the optimum. In other words, the objective function $U(S(\boldsymbol{x}))$ will not be distorted if the frequency misalignment is sufficiently small. This is, of course, under the assumption that the design satisfying $f_r(\boldsymbol{x}) \leq f_{r.\max}$ is attainable. It should also be noted that the regularization factor is continuously differentiable as a function of f_r, so it is suitable for use with gradient-based optimization algorithms.

Figure 1(c) illustrates the effects of regularization for the branch-line coupler example considered in Fig. 1(a)-(b). The profile of the objective function has been modified significantly as compared to the original formulation (3)-(5). Furthermore, the regularized objective function is monotonic along the line segment parameterized by t, therefore, the optimum design is attainable through local search. On the other hand, the location of the optimum designs according to the original and regularized objective functions are identical.

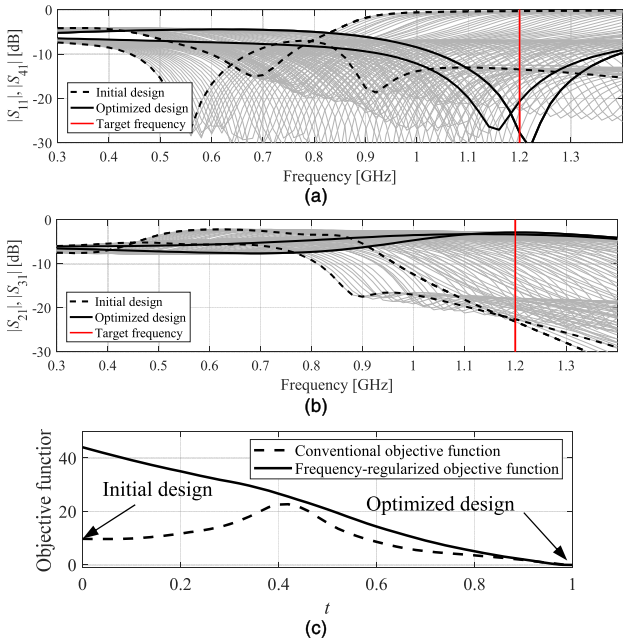

FIGURE 1. Frequency-related regularization: (a), (b) example initial design for a branch-line coupler of Section III (thick dashed line), design optimized for the target frequency 1.2 GHz (thick solid line), as well as the coupler responses (reflection, isolation – top, transmission – bottom) along the line segment that connects the two designs, parameterized by $0 \le t \le 1$ (gray lines); (c) conventional objective function (3)-(5) (- - -) and frequency-regularized objective function (6) with the regularization function (7) (—) versus parameter t. Note the monotonicity of the regularized objective function, which makes the optimum design attainable from the shown initial point even when using a local optimization algorithm. It may not be possible to find the optimum using conventional formulation (3)-(5) due to the objective function profile.

A separate issue is a particular definition of the regularization function, which very much depends on the type of the circuit response. In this work, we focus on miniaturized microwave couplers, so the definition of the function f_r will be illustrated for this case. As the operating frequency of the coupler is primarily related to the minima of the reflection and isolation responses $|S_{11}|$ and $|S_{41}|$, respectively, it is convenient to define the regularization function as follows

$$f_r(\boldsymbol{x}) = \left\| \begin{bmatrix} f_0 \\ f_0 \end{bmatrix} - \begin{bmatrix} f_{\min.S11} \\ f_{\min.S41} \end{bmatrix} \right\| \tag{7}$$

where $f_{\min.S11}$ and $f_{\min.S41}$ are the frequencies corresponding to the mentioned minima of the reflection and isolation characteristics. This information can be readily extracted from EM-simulated coupler responses. A remark should be made that the proposed regularization approach is capable of handling several different minima at different target frequencies. This may be necessary e.g., when optimizing e.g., multi-band transformers and it merely requires to reformulate the regularization function (7). In the reformulated regularization function instead of the frequency vectors of (7), the vector of the target operating frequencies and the vector of the actual resonant frequencies at current design $\boldsymbol{x}$ (that have extracted from the EM-simulated response), respectively, need to be inserted.

C. OPTIMIZATION PROCEDURE

As mentioned before, the frequency-related regularization is pertinent to the formulation of the optimization task but not the specific algorithm utilized to solve it. Thus, it can work with any numerical routine of choice. In this work, we use a trust-region (TR) gradient search [57] with numerical derivatives. TR algorithm is a local procedure, which also gives us an opportunity to demonstrate the advantages of regularization mentioned in Section II.*B*, specifically, the ability of turning a potentially multi-modal problem into a unimodal one.

The trust-region algorithm works by producing a series of approximations $\boldsymbol{x}^{(i)}$, $i = 0, 1, \ldots$, of the optimum design $\boldsymbol{x}^*$ as

$$\boldsymbol{x}^{(i+1)} = \arg \min_{\boldsymbol{x};\, -\boldsymbol{d}^{(i)} \le \boldsymbol{x}-\boldsymbol{x}^{(i)} \le \boldsymbol{d}^{(i)}} U_r(S_L^{(i)}(\boldsymbol{x})) \tag{8}$$

In (8), the modified merit function $U_r(S_L^{(i)})$ is given by (6), and $\boldsymbol{d}^{(i)}$ refers to the search region size vector; the inequalities $-\boldsymbol{d}^{(i)} \le \boldsymbol{x} - \boldsymbol{x}^{(i)} \le \boldsymbol{d}^{(i)}$ in (8) are understood component-wise. Whereas $S_L^{(i)}$ is the first-order Taylor model of $S(\boldsymbol{x})$

$$S_L^{(i)}(\boldsymbol{x}) = S(\boldsymbol{x}^{(i)}) + \boldsymbol{J}_S^{(i)} \cdot (\boldsymbol{x} - \boldsymbol{x}^{(i)}) \tag{9}$$

with $\boldsymbol{J}_S^{(i)}$ being the Jacobian matrix of $S(\boldsymbol{x})$ at $\boldsymbol{x}^{(i)}$, estimated using finite differentiation and $U_r(S(\boldsymbol{x}))$ is defined by (6).

The Jacobian $\boldsymbol{J}_S$ is estimated using finite differentiation. The trust region size vector $\boldsymbol{d}^{(i)}$ is updated after each iteration based on the quality of predictions made by the linear model, i.e., the gain ratio $r = [U_r(S(\boldsymbol{x}^{(i+1)})) - U_r(S(\boldsymbol{x}^{(i)}))]/[U_r(S_L^{(i)}(\boldsymbol{x}^{(i+1)})) - U_r(S_L^{(i)}(\boldsymbol{x}^{(i)}))]$ (recall that $S(\boldsymbol{x})$ represents EM-simulated S-parameters of the circuit under design), i.e., the ratio between the actual and predicted (by the linear model S_L) improvement of the objective function. If $r > 0.75$, we set $\boldsymbol{d}^{(i+1)} = 2\boldsymbol{d}^{(i)}$, whereas if $r < 0.25$, $\boldsymbol{d}^{(i+1)} = \boldsymbol{d}^{(i)}/3$ [58]. It should be noted that the conventional TR procedure can be accelerated using adjoint sensitivities (if available) [32] or by means of sparse sensitivity updates (e.g., [35], [59]). Notwithstanding, this work is focused on investigating the advantages of regularization, especially in terms of improving the optimization process reliability. Reduction of the optimization cost is of secondary importance here. The algorithm is terminated if either of the two conditions is satisfied: $||\boldsymbol{d}^{(i)}|| \le \varepsilon$ or $||\boldsymbol{x}^{(i+1)} - \boldsymbol{x}^{(i)}|| \le \varepsilon$, where ε is a user-defined threshold (in our numerical experiments the value $\varepsilon = 10^{-3}$ was used).

D. TR-BASED OPTIMIZATION WITH REGULARIZATION: ALGORITHM FLOW

Figure 2 shows the flow diagram of the entire procedure. The left panel is essentially the trust-region gradient-based optimization procedure, which, for the sake of evaluating the design quality uses the regularized objective function calculated based on the original function $U(S(\boldsymbol{x}))$ as well as the function f_r computed based on frequency-related information extracted from the EM-simulated response of the device under design.

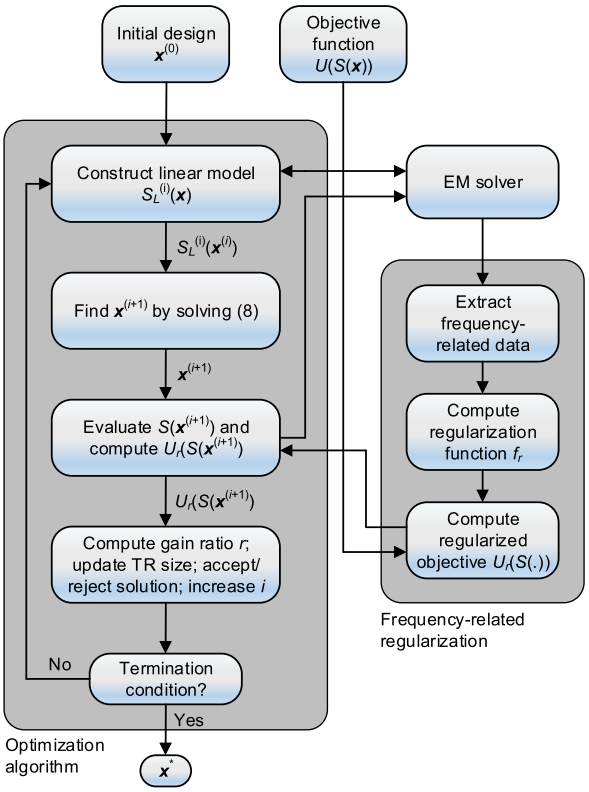

FIGURE 2. Flow diagram of the optimization procedure involving frequency-related regularization.

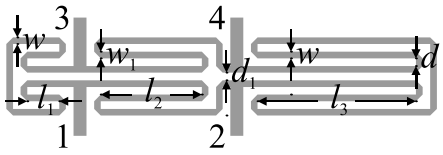

FIGURE 3. Verification case 1: miniaturized microstrip rat-race coupler (RRC) [60].

III. VERIFICATION AND BENCHMARKING

In this section, we illustrate the operation and performance of the proposed methodology using two microstrip couplers: a rat-race, and a branch-line one, shown in Figs. 3 and 4, respectively. The emphasis of the numerical experiments is put on the comparison between the conventional formulations of the optimization problem (cf. Section II.*A*) and the one employing regularization (cf. Section II.*B*). The primary aspect of the algorithmic performance investigated here is reliability of the optimization process, i.e., the ability to identify satisfactory design.

A. CASE 1: COMPACT RAT-RACE COUPLER (RRC)

Our first example is a compact microstrip rat-race coupler (RRC) [60], implemented on RF-35 substrate ($\varepsilon_r = 3.5$, $h = 0.762$ mm, $\tan\delta = 0.0018$). Figure 3 shows the geometry of the circuit. The design variables are $\boldsymbol{x} = [l_1\ l_2\ l_3\ d\ w\ w_1]^T$. Other dimensions are fixed: $d_1 = d + |w - w_1|$, $d = 1.0$, $w_0 = 1.7$, and $l_0 = 15$. The unit for all parameters is mm.

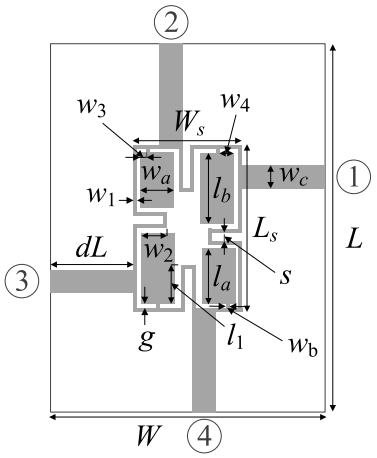

FIGURE 4. Verification case 2: miniaturized branch-line coupler (BLC) [61]. The circuit ports marked using numbered circles.

The computational model of the structure is implemented in CST Microwave Studio.

The optimization goal is to adjust the coupler parameters so that it operates at the frequency f_0 in the following sense:

- The matching and isolation are better than -20 dB at f_0,
- The power split bandwidth defined as the maximum (continuous) range of frequencies symmetric with respect to f_0 for which $d_S(\boldsymbol{x}, f) = ||S_{21}(\boldsymbol{x}, f)| - |S_{31}(\boldsymbol{x}, f)|| \leq 0.5$ dB, is maximized.

In our experiments, the conventional objective function is (3)-(5) (Section II.*A*), whereas the regularization function f_r and the regularized objective U_r are defined as in (7) and (6), respectively (Section II.*B*). The coupler was optimized from three different initial designs, in each case, optimization was performed for two different target operating frequencies. All initial designs are detuned, in particular, the power split error largely exceeds the acceptance value of 0.5 dB. Table 1, as well as Figs. 5 and 6 show the results obtained using the algorithm of Section II.*C* and the conventional objective function as well as frequency-related regularization proposed in this work.

It can be observed that the optimization process involving conventional formulation failed to find satisfactory designs (i.e., featuring non-zero power split bandwidth) in half of the test cases. On the other hand, the algorithm equipped with the proposed regularization scheme managed to find good designs in all six cases. Furthermore, the power split bandwidth is considerably wider for the designs obtained using regularization than for conventional approach. The average optimization cost in the case of the conventional framework is around 53 EM analyzes, whereas it slightly exceeds 57 for the proposed technique. Thus, the computational complexity of both approaches is comparable. In other words, regularization leads to significant improvement of the optimization process reliability without compromising the efficiency. It should be emphasized that similarity of the optimization cost for the standard TR search and the process employing regularization

TABLE 1. Optimization results for compact RRC of Fig. 3.

Operating frequency of the initial design[$] [GHz]	Target operating frequency f_0 [GHz]	Performance figures: Conventional formulation (3)-(5) Power split bandwidth	Performance figures: Frequency regularization (6), (7) [this work] Power split bandwidth
1.8	1.0	0[#]	0.26
	2.0	0.55	0.63
1.5	1.3	0.35	0.42
	1.8	0[#]	0.40
1.9	1.0	0[#]	0.13
	1.3	0.28	0.39

[$] Roughly assessed operating frequencies of the initial designs.
[#] The algorithm failed to find a satisfactory design.

TABLE 2. Optimization results for compact BLC of Fig. 4.

Operating frequency of the initial design[$] [GHz]	Target operating frequency f_0 [GHz]	Performance figures: Conventional formulation (3)-(5) Power split bandwidth	Performance figures: Frequency regularization (6), (7) [this work] Power split bandwidth
0.7		0[#]	0.05
1.4	1.0	0.20	0.37
1.5		0[#]	0.26
1.4	0.8	0.26	0.15
1.2	1.5	0.13	0.17
1.5	1.8	0.38	0.75

[$] Roughly assessed operating frequencies of the initial designs.
[#] The algorithm failed to find a satisfactory design.

was to be expected because both methods use the same underlying optimization engine ((8) and (9)).

Although the functional landscape of the regularized objective function is smoother than for the standard formulation, which should lead to a certain speedup, regularization-based algorithm typically runs for a similar number of iterations due to identifying higher-quality final designs (which require longer exploration of the parameter space).

B. CASE 2: MINIATURIZED BRANCH-LINE COUPLER (BLC)

The second example is a compact branch line coupler [61], shown in Fig. 4. The circuit is implemented on RO4003 substrate ($\varepsilon_r = 3.38$, $h = 0.51$ mm, $\tan\delta = 0.0027$). The design variables are $\boldsymbol{x} = [g\ l_{1r}\ l_a\ l_b\ w_1\ w_{2r}\ w_{3r}\ w_{4r}\ w_a\ w_b]^T$. Other parameters are described by the following relations: $L = 2dL + L_s$, $L_s = 4w_1 + 4g + s + l_a + l_b$, $W = 2dL + W_s$, $W_s = 4w_1 + 4g + s + 2w_a$, $l_1 = l_b l_{1r}$, $w_2 = w_a w_{2r}$, $w_3 = w_{3r} w_a$, and $w_4 = w_{4r} w_a$. All dimensions are expressed in mm except those with r-subscript which are relative. The computational model of the structure is implemented in CST Microwave Studio.

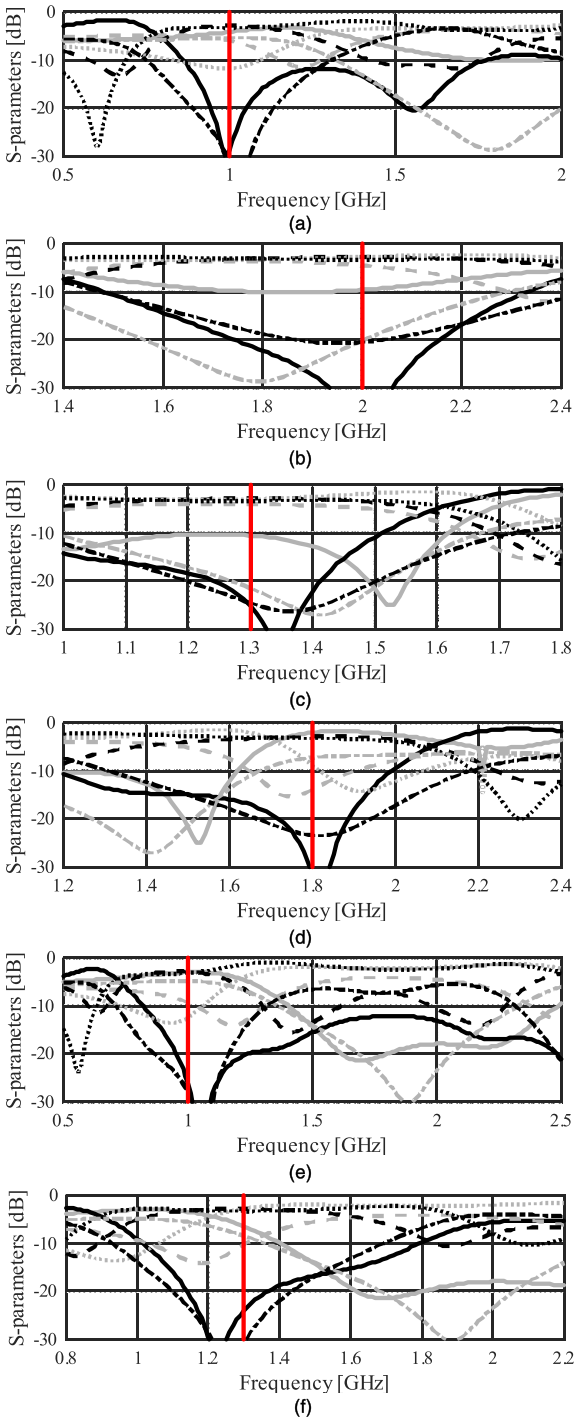

FIGURE 5. Optimized designs of miniaturized rat-race coupler of Fig. 3 obtained using the proposed regularization scheme (black) starting from the initial designs of Table 1 (gray) for different values of the target operating frequencies: (a) $f_0 = 1.0$ GHz, (b) $f_0 = 2.0$ GHz, (c) $f_0 = 1.3$ GHz, (d) $f_0 = 1.8$ GHz, (e) $f_0 = 1.0$ GHz, and (f) $f_0 = 1.3$ GHz. Shown are the S-parameters of RRC: S_{11} (–), S_{21} (––), S_{31} (. . .), and S_{41} (–.).

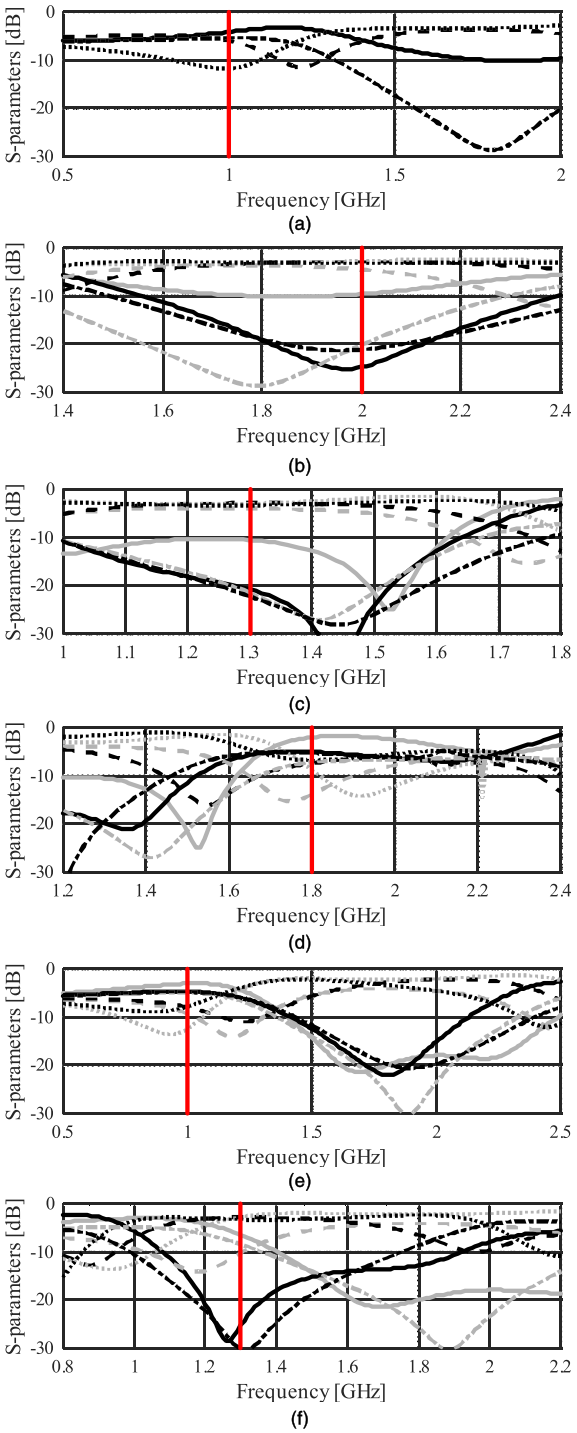

FIGURE 6. Optimized designs of miniaturized rat-race coupler of Fig. 3 obtained conventional objective function (3)-(5) (black) starting from the initial designs of Table 1 (gray) for different values of the target operating frequencies: (a) $f_0 = 1.0$ GHz, (b) $f_0 = 2.0$ GHz, (c) $f_0 = 1.3$ GHz, (d) $f_0 = 1.8$ GHz, (e) $f_0 = 1.0$ GHz, and (f) $f_0 = 1.3$ GHz. Shown are the S-parameters of RRC: S_{11} (–), S_{21} (––), S_{31} (. . .), and S_{41} (–.). Observe that in Fig. 6(a), the conventional optimization process got stuck in the initial design, which is not the case for the proposed regularization algorithm (cf. Fig. 5(a)).

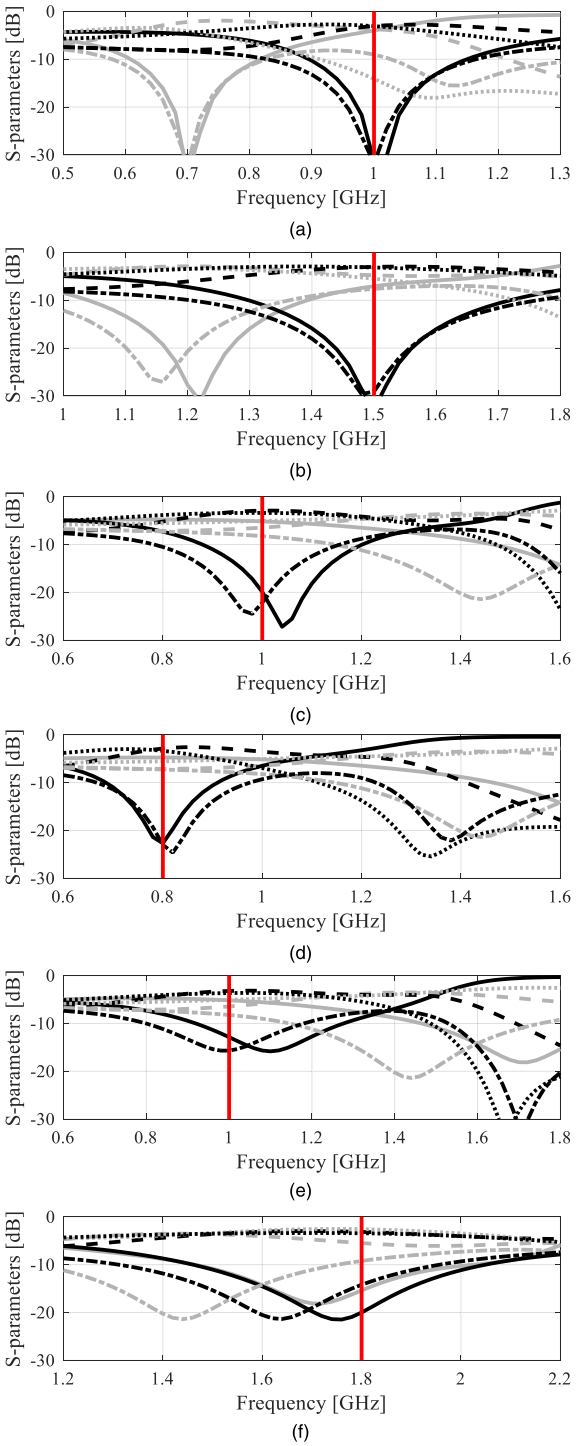

FIGURE 7. Optimized designs of miniaturized branch-line coupler of Fig. 4 obtained using the proposed regularization scheme (black) starting from the initial designs of Table 2 (gray) for different values of the target operating frequencies: (a) $f_0 = 1.0$ GHz, (b) $f_0 = 1.5$ GHz, (c) $f_0 = 1.0$ GHz, (d) $f_0 = 0.8$ GHz, (e) $f_0 = 1.0$ GHz, and (f) $f_0 = 1.8$ GHz. Shown are the S-parameters of BLC: S_{11} (–), S_{21} (––), S_{31} (. . .), and S_{41} (–.).

The design objectives are the same as for the previous example, i.e., given a target operating frequency f_0, the coupler matching and isolation are supposed to be equal or better than -20 dB (at f_0), and the power split bandwidth (defined for $d_S(\boldsymbol{x}, f) = ||S_{21}(\boldsymbol{x}, f)| - |S_{31}(\boldsymbol{x}, f)|| \leq 0.5$ dB) is to be maximized. We use (3)-(5) as the conventional objective function, and (6), (7) as the regularized cost function.

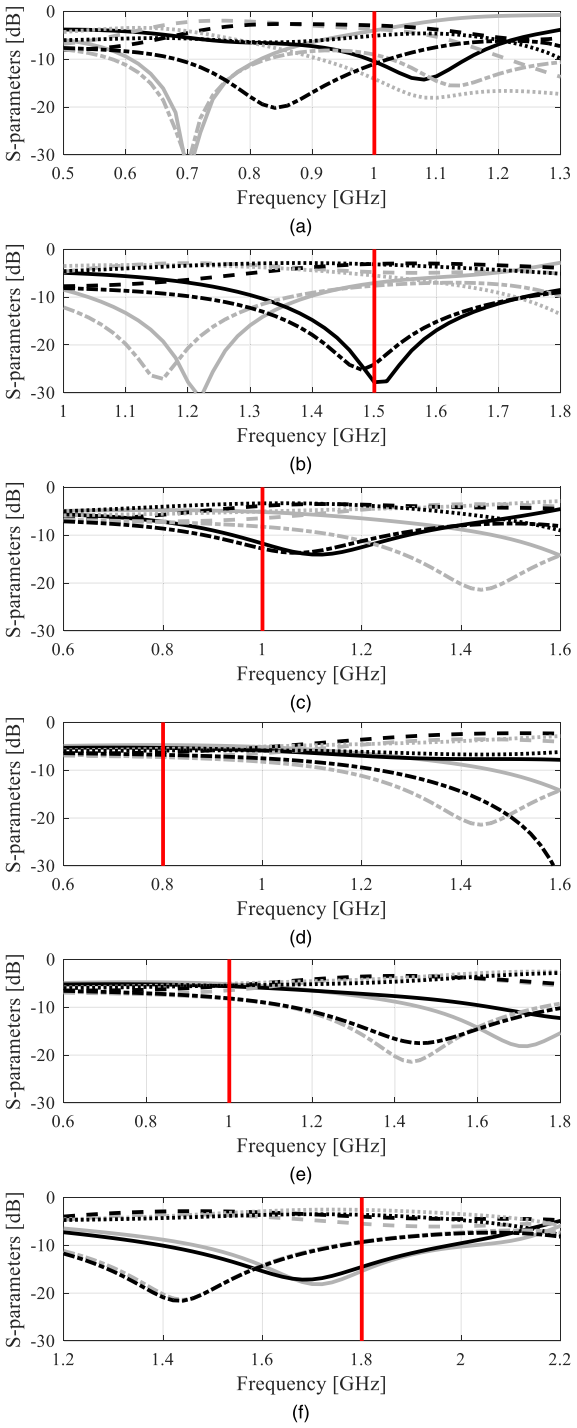

FIGURE 8. Optimized designs of miniaturized branch-line coupler of Fig. 4 obtained conventional objective function (3)-(5) (black) starting from the initial designs of Table 2 (gray) for different values of the target operating frequencies: (a) $f_0 = 1.0$ GHz, (b) $f_0 = 1.5$ GHz, (c) $f_0 = 1.0$ GHz, (d) $f_0 = 0.8$ GHz, (e) $f_0 = 1.0$ GHz, and (f) $f_0 = 1.8$ GHz. Shown are the S-parameters of BLC: S_{11} (–), S_{21} (– –), S_{31} (. . .), and S_{41} (–.).

The numerical experiments were arranged similarly as in Section III.*A* and the results have been gathered in Table 2. The coupler was optimized starting from several different initial designs (cf. Table 2) and for four different target operating frequencies $f_0 = 1.0$ GHz (starting from around 0.7 GHz, 1.4 GHz and 1.5 GHz), as well as $f_0 = 0.8$ GHz, 1.5 GHz, and 1.8 GHz (each starting from a separate starting point as reported in Table 2). The initial and optimized designs obtained within the proposed regularization-based framework and conventional one are shown in Figs. 7 and 8, respectively. The results are consistent with those obtained for the first example. In particular, regularization ensures identification of good designs for all considered scenarios, which is not the case for the conventional formulation (fails in two out of six cases). Also, the power split bandwidth obtained with regularization is broader in all but one case than for the conventional setup. Finally, the computational costs are similar in both cases (average of 72 and 77 EM analyses for conventional and regularization formulations, respectively).

IV. CONCLUSION

The paper discussed a frequency-related regularization technique for improved-reliability design optimization of microwave passive components. The presented methodology aims at enforcing the proper alignment between actual and the target operating frequency (or frequencies) of the structure under design, which is realized by introducing a regularization term the penalizes the aforementioned discrepancies. The primary benefit of this approach is to smoothen the objective function landscape and to make it monotonic with respect to frequency relocations. This greatly facilitates redesigning microwave components to different operating conditions as well as their reliable optimization when the initial design is of poor quality. At the same time, it reduces the need for global search routines, which are normally applied in such cases. In particular, in many practical cases, structure re-design over broad ranges of operating conditions would require the employment of stochastic techniques, such as nature-inspired population-based methods, which would entail considerable computational expenses and reduce the robustness of the optimization process because the aforementioned techniques exhibit limited repeatability of solutions.

The proposed technique has been comprehensively validated using two miniaturized couplers, a rat-race and a branch-line one. Their geometry parameter tuning was carried out under different scenarios, using several the target operating frequencies and initial designs. The results clearly demonstrate the advantages of regularization with satisfactory designs obtained for all considered cases, as opposed to conventional formulation, which failed in a significant number of scenarios featuring the initial design of insufficient quality. At the same time, the average computational cost of the optimization process with regularization is comparable to the standard case. The proposed technique can be a useful enhancement of simulation-driven optimization routines, especially in situations when the improvement of reliability and computational efficiency is of concern.

Potential limitations of the presented approach are twofold. On the one hand, although regularization considerably increases the range of frequency relocation that can be

realized when coupling it with local search techniques, the method is likely to fail in some extreme cases that may still require globalized optimization procedures. On the other hand, in some cases, especially wideband responses, the very definition of the regularization function may not be straightforward, and appropriate generalizations may be required to broaden the scope of possible applications of the approach. Both aspects will be investigated as a part of future research.

ACKNOWLEDGMENT

The authors would like to thank Dassault Systemes, France, for making CST Microwave Studio available.

REFERENCES

[1] T. Su, S.-J. Wang, Y.-L. Zhang, Z.-P. Li, and L.-J. Zhang, "A compact DBR filter using Π-network and dual-line equivalent circuit," *IEEE Microw. Wireless Compon. Lett.*, vol. 23, no. 7, pp. 350–352, Jul. 2013.

[2] S. P. Savaidis, Z. C. Ioannidis, S. A. Mitilineos, and N. A. Stathopoulos, "Design of waveguide microwave pulse compressors using equivalent circuits," *IEEE Trans. Microw. Theory Techn.*, vol. 63, no. 1, pp. 125–134, Jan. 2015.

[3] L. Zappelli, "Equivalent circuits of lossy two-port waveguide devices," *IEEE Trans. Microw. Theory Techn.*, vol. 67, no. 10, pp. 4095–4106, Oct. 2019.

[4] Y. Karisan, C. Caglayan, G. C. Trichopoulos, and K. Sertel, "Lumped-element equivalent-circuit modeling of millimeter-wave HEMT parasitics through full-wave electromagnetic analysis," *IEEE Trans. Microw. Theory Techn.*, vol. 64, no. 5, pp. 1419–1430, May 2016.

[5] M. Nosrati, Z. Abbasi, M. Baghelani, S. Bhadra, and M. Daneshmand, "Locally strong-coupled microwave resonator using PEMC boundary for distant sensing applications," *IEEE Trans. Microw. Theory Techn.*, vol. 67, no. 10, pp. 4130–4139, Oct. 2019.

[6] P. Zhou, L. Wang, G. Zhang, J. Jiang, H. Chen, Y. Zhou, D. Liang, and L. Deng, "A stretchable metamaterial absorber with deformation compensation design at microwave frequencies," *IEEE Trans. Antennas Propag.*, vol. 67, no. 1, pp. 291–297, Jan. 2019.

[7] W. Yu, Y. Rao, H. J. Qian, and X. Luo, "Reflectionless filtering 90° coupler using stacked cross coupled-line and loaded cross-stub," *IEEE Microw. Wireless Compon. Lett.*, vol. 30, no. 5, pp. 481–484, May 2020.

[8] H. Jia and R. R. Mansour, "An efficient technique for tuning and design of filters and diplexers," *IEEE Trans. Microw. Theory Techn.*, vol. 68, no. 7, pp. 2610–2624, Jul. 2020.

[9] P. Manfredi and F. G. Canavero, "Efficient statistical simulation of microwave devices via stochastic testing-based circuit equivalents of nonlinear components," *IEEE Trans. Microw. Theory Techn.*, vol. 63, no. 5, pp. 1502–1511, May 2015.

[10] S. Koziel and J. W. Bandler, "Rapid yield estimation and optimization of microwave structures exploiting feature-based statistical analysis," *IEEE Trans. Microw. Theory Techn.*, vol. 63, no. 1, pp. 107–114, Jan. 2015.

[11] J. Zhang, F. Feng, W. Na, S. Yan, and Q. Zhang, "Parallel space-mapping based yield-driven EM optimization incorporating trust region algorithm and polynomial chaos expansion," *IEEE Access*, vol. 7, pp. 143673–143683, 2019.

[12] S. Koziel and A. T. Sigurôsson, "Performance-driven modeling of compact couplers in restricted domains," *Int. J. RF Microw. Comput.-Aided Eng.*, vol. 28, no. 6, Aug. 2018, Art. no. e21296.

[13] D. Letavin, "Miniature microstrip branch line coupler with folded artificial transmission lines," *AEU - Int. J. Electron. Commun.*, vol. 99, pp. 8–13, Feb. 2019.

[14] Z. Qian and J. Chen, "Compact bandpass filter using CMRC-based dual-behavior resonator," *Int. J. RF Microw. Comput.-Aided Eng.*, vol. 29, no. 7, Jul. 2019, Art. no. e21719.

[15] S. Chen, M. Guo, K. Xu, P. Zhao, L. Dong, and G. Wang, "A frequency synthesizer based microwave permittivity sensor using CMRC structure," *IEEE Access*, vol. 6, pp. 8556–8563, 2018.

[16] V.-M.-R. Gongal-Reddy, S. Zhang, C. Zhang, and Q.-J. Zhang, "Parallel computational approach to gradient based EM optimization of passive microwave circuits," *IEEE Trans. Microw. Theory Techn.*, vol. 64, no. 1, pp. 44–59, Jan. 2016.

[17] S. Koziel, "Computationally efficient multi-fidelity multi-grid design optimization of microwave structures," *Appl. Comput. Electromagn. Soc. J.*, vol. 25, no. 7, pp. 578–586, 2010.

[18] X. Li and K. M. Luk, "The grey wolf optimizer and its applications in electromagnetics," *IEEE Trans. Antennas Propag.*, vol. 68, no. 3, pp. 2186–2197, Mar. 2020.

[19] E. Yigit and H. Duysak, "Determination of optimal layer sequence and thickness for broadband multilayer absorber design using double-stage artificial bee colony algorithm," *IEEE Trans. Microw. Theory Techn.*, vol. 67, no. 8, pp. 3306–3317, Aug. 2019.

[20] A. A. Al-Azza, A. A. Al-Jodah, and F. J. Harackiewicz, "Spider monkey optimization: A novel technique for antenna optimization," *IEEE Antennas Wireless Propag. Lett.*, vol. 15, pp. 1016–1019, 2016.

[21] M.-C. Tang, X. Chen, M. Li, and R. W. Ziolkowski, "Particle swarm optimized, 3-D-printed, wideband, compact hemispherical antenna," *IEEE Antennas Wireless Propag. Lett.*, vol. 17, no. 11, pp. 2031–2035, Nov. 2018.

[22] A. Toktas, D. Ustun, and M. Tekbas, "Multi-objective design of multi-layer radar absorber using surrogate-based optimization," *IEEE Trans. Microw. Theory Techn.*, vol. 67, no. 8, pp. 3318–3329, Aug. 2019.

[23] F. Gunes, A. Uluslu, and P. Mahouti, "Pareto optimal characterization of a microwave transistor," *IEEE Access*, vol. 8, pp. 47900–47913, 2020.

[24] Y. Zhao and G. Wang, "Multi-objective optimisation technique for coupling matrix synthesis of lossy filters," *IET Microw., Antennas Propag.*, vol. 7, no. 11, pp. 926–933, Aug. 2013.

[25] D. I. L. de Villiers and S. M. Koziel, "Fast multi-objective optimisation of pencil beam reflector antenna radiation pattern responses using Kriging," *IET Microw., Antennas Propag.*, vol. 12, no. 1, pp. 120–126, Jan. 2018.

[26] A. K. Prasad, M. Ahadi, and S. Roy, "Multidimensional uncertainty quantification of microwave/RF networks using linear regression and optimal design of experiments," *IEEE Trans. Microw. Theory Techn.*, vol. 64, no. 8, pp. 2433–2446, Aug. 2016.

[27] A. Petrocchi, A. Kaintura, G. Avolio, D. Spina, T. Dhaene, A. Raffo, and D. M. M.-P. Schreurs, "Measurement uncertainty propagation in transistor model parameters via polynomial chaos expansion," *IEEE Microw. Wireless Compon. Lett.*, vol. 27, no. 6, pp. 572–574, Jun. 2017.

[28] J. S. Ochoa and A. C. Cangellaris, "Random-space dimensionality reduction for expedient yield estimation of passive microwave structures," *IEEE Trans. Microw. Theory Techn.*, vol. 61, no. 12, pp. 4313–4321, Dec. 2013.

[29] J. E. Rayas-Sanchez and V. Gutierrez-Ayala, "EM-based Monte Carlo analysis and yield prediction of microwave circuits using linear-input neural-output space mapping," *IEEE Trans. Microw. Theory Techn.*, vol. 54, no. 12, pp. 4528–4537, Dec. 2006.

[30] S. H. Hall and H. L. Heck, *Advanced Signal Integrity for High-Speed Digital Designs*. Hoboken, NJ, USA: Wiley, 2009.

[31] Y. Dong, M. Tang, P. Li, and J. Mao, "Transient electromagnetic-thermal simulation of dispersive media using DGTD method," *IEEE Trans. Electromagn. Compat.*, vol. 61, no. 4, pp. 1305–1313, Aug. 2019.

[32] H. Malhi and M. H. Bakr, "Geometry evolution of microwave filters exploiting self-adjoint sensitivity analysis," in *IEEE MTT-S Int. Microw. Symp. Dig.*, Aug. 2015, pp. 1–3.

[33] E. Hassan, B. Scheiner, F. Michler, M. Berggren, E. Wadbro, F. Rohrl, S. Zorn, R. Weigel, and F. Lurz, "Multilayer topology optimization of wideband SIW-to-waveguide transitions," *IEEE Trans. Microw. Theory Techn.*, vol. 68, no. 4, pp. 1326–1339, Apr. 2020.

[34] S. Koziel and A. Pietrenko-Dabrowska, "Variable-fidelity simulation models and sparse gradient updates for cost-efficient optimization of compact antenna input characteristics," *Sensors*, vol. 19, no. 8, p. 1806, Apr. 2019.

[35] A. Pietrenko-Dabrowska and S. Koziel, "Computationally-efficient design optimisation of antennas by accelerated gradient search with sensitivity and design change monitoring," *IET Microw., Antennas Propag.*, vol. 14, no. 2, pp. 165–170, Feb. 2020.

[36] B. Liu, H. Yang, and M. J. Lancaster, "Global optimization of microwave filters based on a surrogate model-assisted evolutionary algorithm," *IEEE Trans. Microw. Theory Techn.*, vol. 65, no. 6, pp. 1976–1985, Jun. 2017.

[37] S. Koziel and A. Pietrenko-Dabrowska, "Rapid optimization of compact microwave passives using kriging surrogates and iterative correction," *IEEE Access*, vol. 8, pp. 53587–53594, 2020.

[38] Z. Zhang, Q. S. Cheng, H. Chen, and F. Jiang, "An efficient hybrid sampling method for neural network-based microwave component modeling and optimization," *IEEE Microw. Wireless Compon. Lett.*, vol. 30, no. 7, pp. 625–628, Jul. 2020.

[39] S. Koziel and A. T. Sigurôsson, "Multi-fidelity EM simulations and constrained surrogate modelling for low-cost multi-objective design optimisation of antennas," *IET Microw., Antennas Propag.*, vol. 12, no. 13, pp. 2025–2029, Oct. 2018.
[40] F. Feng, J. Zhang, W. Zhang, Z. Zhao, J. Jin, and Q.-J. Zhang, "Coarse- and fine-mesh space mapping for EM optimization incorporating mesh deformation," *IEEE Microw. Wireless Compon. Lett.*, vol. 29, no. 8, pp. 510–512, Aug. 2019.
[41] S. Koziel, "Shape-preserving response prediction for microwave design optimization," *IEEE Trans. Microw. Theory Techn.*, vol. 58, no. 11, pp. 2829–2837, Nov. 2010.
[42] M. A. Ismail, D. Smith, A. Panariello, Y. Wang, and M. Yu, "EM-based design of large-scale dielectric-resonator filters and multiplexers by space mapping," *IEEE Trans. Microw. Theory Techn.*, vol. 52, no. 1, pp. 386–392, Jan. 2004.
[43] J. E. Rayas-Sanchez, "Power in simplicity with ASM: Tracing the aggressive space mapping algorithm over two decades of development and engineering applications," *IEEE Microw. Mag.*, vol. 17, no. 4, pp. 64–76, Apr. 2016.
[44] Y. Su, J. Li, Z. Fan, and R. Chen, "Shaping optimization of double reflector antenna based on manifold mapping," in *Proc. Int. Appl. Comp. Electromagn. Symp. (ACES)*, Suzhou, China, Aug. 2017, pp. 1–2.
[45] S. Koziel and S. D. Unnsteinsson, "Expedited design closure of antennas by means of Trust-Region-Based adaptive response scaling," *IEEE Antennas Wireless Propag. Lett.*, vol. 17, no. 6, pp. 1099–1103, Jun. 2018.
[46] B. Xia, Z. Ren, and C.-S. Koh, "Utilizing kriging surrogate models for multi-objective robust optimization of electromagnetic devices," *IEEE Trans. Magn.*, vol. 50, no. 2, pp. 693–696, Feb. 2014.
[47] A. M. Alzahed, S. M. Mikki, and Y. M. M. Antar, "Nonlinear mutual coupling compensation operator design using a novel electromagnetic machine learning paradigm," *IEEE Antennas Wireless Propag. Lett.*, vol. 18, no. 5, pp. 861–865, May 2019.
[48] H. M. Torun and M. Swaminathan, "High-dimensional global optimization method for high-frequency electronic design," *IEEE Trans. Microw. Theory Techn.*, vol. 67, no. 6, pp. 2128–2142, Jun. 2019.
[49] S. Xiao, G. Q. Liu, K. L. Zhang, Y. Z. Jing, J. H. Duan, P. Di Barba, and J. K. Sykulski, "Multi-objective Pareto optimization of electromagnetic devices exploiting kriging with lipschitzian optimized expected improvement," *IEEE Trans. Magn.*, vol. 54, no. 3, pp. 1–4, Mar. 2018.
[50] J. Du and C. Roblin, "Statistical modeling of disturbed antennas based on the polynomial chaos expansion," *IEEE Antennas Wireless Propag. Lett.*, vol. 16, pp. 1843–1847, 2017.
[51] S. Koziel and A. Pietrenko-Dabrowska, "Expedited feature-based quasi-global optimization of multi-band antenna input characteristics with jacobian variability tracking," *IEEE Access*, vol. 8, pp. 83907–83915, 2020.
[52] S. Koziel, "Fast simulation-driven antenna design using response-feature surrogates," *Int. J. RF Microw. Comput.-Aided Eng.*, vol. 25, no. 5, pp. 394–402, Jun. 2015.
[53] F. Feng, C. Zhang, W. Na, J. Zhang, W. Zhang, and Q.-J. Zhang, "Adaptive feature zero assisted surrogate-based EM optimization for microwave filter design," *IEEE Microw. Wireless Compon. Lett.*, vol. 29, no. 1, pp. 2–4, Jan. 2019.
[54] S. Koziel and S. Ogurtsov, "Rapid design closure of linear microstrip antenna array apertures using response features," *IEEE Antennas Wireless Propag. Lett.*, vol. 17, no. 4, pp. 645–648, Apr. 2018.
[55] F. Ferranti, Y. Rolain, L. Knockaert, and T. Dhaene, "Variance weighted vector fitting for noisy frequency responses," *IEEE Microw. Wireless Compon. Lett.*, vol. 20, no. 4, pp. 187–189, Apr. 2010.
[56] H. Zhu and A. M. Abbosh, "A compact tunable directional coupler with continuously tuned differential phase," *IEEE Microw. Wireless Compon. Lett.*, vol. 28, no. 1, pp. 19–21, Jan. 2018.
[57] A. R. Conn, N. I. M. Gould, and P. L. Toint, *Trust Region Methods* (MPS-SIAM Series on Optimization). Philadelphia, PA, USA: SIAM, 2000. [Online]. Available: https://epubs.siam.org/doi/book/10.1137/1.9780898719857?mobileUi=0, doi: 10.1137/1.9780898719857.
[58] S. Koziel, J. W. Bandler, and Q. S. Cheng, "Robust trust-region space-mapping algorithms for microwave design optimization," *IEEE Trans. Microw. Theory Techn.*, vol. 58, no. 8, pp. 2166–2174, Aug. 2010.
[59] S. Koziel and A. Pietrenko-Dabrowska, "Efficient gradient-based algorithm with numerical derivatives for expedited optimization of multi-parameter miniaturized impedance matching transformers," *Radioengineering*, vol. 27, no. 3, pp. 572–578, Sep. 2019.
[60] S. Koziel and A. Pietrenko-Dabrowska, "Reduced-cost surrogate modelling of compact microwave components by two-level kriging interpolation," *Eng. Optim.*, vol. 52, no. 6, pp. 960–972, Jun. 2020.
[61] C.-H. Tseng and C.-L. Chang, "A rigorous design methodology for compact planar branch-line and rat-race couplers with asymmetrical T-Structures," *IEEE Trans. Microw. Theory Techn.*, vol. 60, no. 7, pp. 2085–2092, Jul. 2012.

SLAWOMIR KOZIEL (Senior Member, IEEE) received the M.Sc. and Ph.D. degrees in electronic engineering from the Gdansk University of Technology, Poland, in 1995 and 2000, respectively, and the M.Sc. degrees in theoretical physics and in mathematics and the Ph.D. degree in mathematics from the University of Gdansk, Poland, in 2000, 2002, and 2003, respectively. He is currently a Professor with the Department of Engineering, Reykjavik University, Iceland. His research interests include CAD and modeling of microwave and antenna structures, simulation-driven design, surrogate-based optimization, space mapping, circuit theory, analog signal processing, evolutionary computation, and numerical analysis.

ANNA PIETRENKO-DABROWSKA (Senior Member, IEEE) received the M.Sc. and Ph.D. degrees in electronic engineering from the Gdansk University of Technology, Poland, in 1998 and 2007, respectively. She is currently an Associate Professor with the Gdansk University of Technology. Her research interests include simulation-driven design, design optimization, control theory, modeling of microwave and antenna structures, and numerical analysis.

MUATH AL-HASAN (Senior Member, IEEE) received the B.Sc. degree in electrical engineering from the Jordan University of Science and Technology, Jordan, in 2005, the M.Sc. degree in wireless communications from Yarmouk University, Jordan, in 2008, and the Ph.D. degree in telecommunication engineering from the Institut National de la Recherche Scientifique (INRS), Université du Québec, Canada, 2015. From 2013 to 2014, he was with Planets Inc., California, USA. In May 2015, he joined Concordia University, Montréal, QC H3G 1M8, Canada, as Postdoctoral Fellowship. He is currently an Assistant Professor with Al Ain University, United Arab Emirates. His current research interests include antenna design at millimeter-wave and Terahertz, channel measurements in multiple-input and multiple-output (MIMO) systems, and machine learning and artificial intelligence in antenna design.